

AN EXPERIENCE OF USING NUMERICAL METHODS IN EXPERIMENTAL INVESTIGATIONS OF TSAGI

S.M.Bosnyakov*, A.R.Gorbushin*, S.V.Mikhaylov*, V.Ya.Neyland*

***Central Aerohydrodynamic Institute (TsAGI), Zhukovsky, Russia**

bosnyakov@tsagi.ru; gorbushin@tsagi.ru; sergey.mikhaylov@tsagi.ru; neyland@tsagi.ru

Keywords: *numerical simulation, wind tunnel, boundary conditions, perforation, slotted walls.*

Abstract

Description of EWT (Electronic Wind Tunnel) code is done. This code is used in TsAGI from 1996. It permits to solve stationary (RANS) and non-stationary (URANS) Navier-Stokes equations with Reynolds-averaging. A possibility to simulate large-scale vortices (LES) is realized. Special boundary conditions, such as “wind tunnel start”, “permeable walls” (perforated and slotted), “threadmill” and “plenum chamber walls” are discussed in details. It is mentioned that code effectively uses chimera-type grids based on original “connect” technology. Practical aspects are described. It is shown that grid templates with special blocks for model and wind tunnel parts are prepared in advance. It permits to change model in EWT operatively. Important algorithm for grid rebuilding, in the case of changing the model incidence and slip angles, is also developed and works reliable.

Initially (1996), the code was adapted for conditions of T-128 wind tunnel (TsAGI). Later on (2006), the version for ETW (European Transonic Windtunnel) appeared. Special code for T-104 wind tunnel (TsAGI) with simulation of “moving runway” and open test section has been developed after that (2008).

Examples of results obtained in the frame of code integration to experimental cycle of different wind tunnels are presented. Important tasks are solved: 1) wall interference prediction; 2) systematic mistakes such as support influence etc. estimation; 3) creation of optimal wind tunnel parts. Picture bellow shows result of penishe height problem solution during mounting the half model in T-128 TsAGI.

Streamlines around “free” model and half-model in wind tunnel are compared.

1 Introduction

Experience of simulating some aspects of the physical experiment in the wind tunnel is of the highest interest. These works were started by TsAGI in the 1980s on the initiative of V.Ya.Neyland (Corresponding Member of the Russian Academy of Sciences) in order to improve the reliability of the aerodynamic characteristics obtained in the TsAGI wind tunnels (WT) for the models of the Buran-Energia aerospace system. For transonic working regimes of the TsAGI T-128 tunnel, it was for the first time [1] that the numerical method developed by Yu.B. Lifshiyz and S.A. Velichko [2] was used to estimate the effect of the tunnel’s perforated walls. This made it possible to establish the procedure for adapting the perforated boundaries of the WT T-128 test section [3]. For subsonic flow regimes, a research team headed by V.M. Neyland has developed procedures for taking into account the effect of perforated boundaries on the aerodynamic characteristics of the models. For the external surface of the boundary layer on the perforated wall the boundary conditions were experimentally found as the Darcy law [4], [5]. In the flow potential core, the Laplace problem was solved (method of singularities [6] and integral method [7]). V.Ya.Neyland proposed in 1992 to develop nonlinear code and take into account influence of wind tunnels walls on results of Tu-144 model tests in T-128 and T-109 TsAGI. It was beginning of Electronic Wind Tunnel (EWT). He is scientific supervisor of this study up today. By means of the EWT software package [8], [9], the limit Mach

number for the applicability of fast linear methods was determined. It was proved that for a moderate degree of the test section blockage the linear methods can be applied up to $M = 0.9$. The methodology for taking into account the effect of boundaries for subsonic velocities of the flow in that form as it is used at present in T-128 is described in details in [10]. Originally, for the determination of the influence of flow boundaries, two basic experimental methods were used: (1) tests of geometrically similar models; (2) tests of the same model in the small and large WT, where the tests in the large wind tunnel were considered as an approximation of infinite flow. In order to find the influence of the support devices, the experimental method of “doubling” was used, when the model was mounted on one sting and tests were made with and without the dummy sting. In order to account for the effect of the flow boundaries and supporting devices the appropriate procedures have been developed. Unfortunately, experimental methods cannot provide reliable data for the case of an isolated model in an infinite flow. This drawback is removed by numerical procedures, the results of which are easily integrated into the available methods to account for the effect of the flow and supporting devices. At present, these works are ongoing. Special codes have been developed to simulate the experiment in TsAGI’s wind tunnel T-104. Interesting results were obtained by the efforts on the creation of the mathematical model of the European Transonic Windtunnel (ETW) with slotted walls [9]. This work was carried out with support from J. Quest, the coordinator of the projects of the European Union. At present, such mathematical models for European wind tunnels are being created in the research centers of Germany, France and Britain, for example, [11], [12], [13].

2. Mathematical Model of WT and its Construction Features

For convenience, all geometrical objects used in the creation of the WT surface mathematical model or of the corresponding model of an aircraft’s surface are divided into compartments. For example, in the case of the aircraft’s

forward fuselage, the flight deck is one compartment and the cylindrical part of the fuselage is another compartment.

The number of compartments depends on the complexity of the object. The procedure consists of several stages and has elements of interactive operation. For example, let’s consider the technology used at TsAGI. As the first step in the design engineering bureau, on the basis of the available drawings, a CAD project of the wind tunnel is created, for example WT T-104. At the second step, the Coons patches [13] are constructed. The patches are clearly seen in Fig. 1.

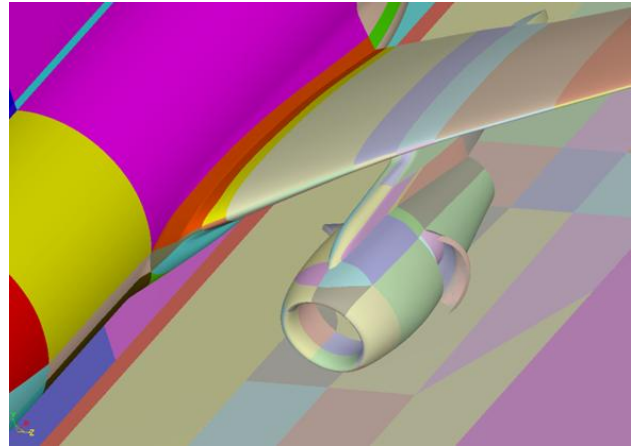


Fig. 1. Mathematical model of the airframe-wing-engine configuration

At the third stage, a computational grid, which has special blocks designed to locate virtual models of aircrafts, is constructed. As an example, we consider a typical case of the arrangement of the model of a passenger aircraft with an engine. A photograph of the experimental unit for Transonic Wind Tunnel with close test section is shown in Fig. 2.

Calculations are performed using a multiblock structured computational grid. Each block is a curvilinear hexahedron (possibly with degenerated boundaries). Mathematical model and blocks structure are illustrated in Fig. 3.

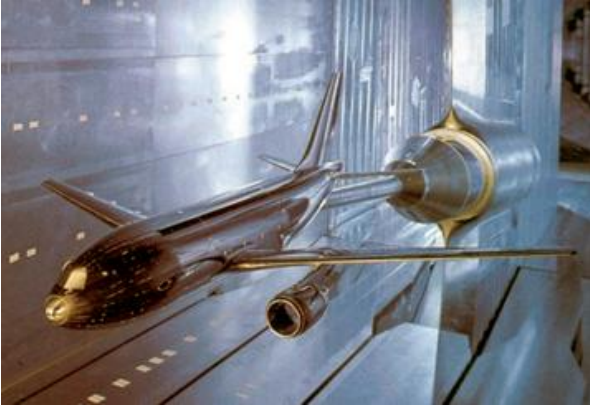


Fig. 2. Model in the Transonic Wind Tunnel

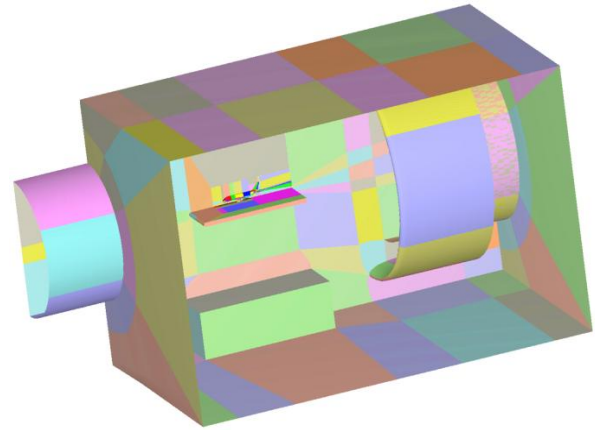


Fig. 5. Block structure of the WT T-104

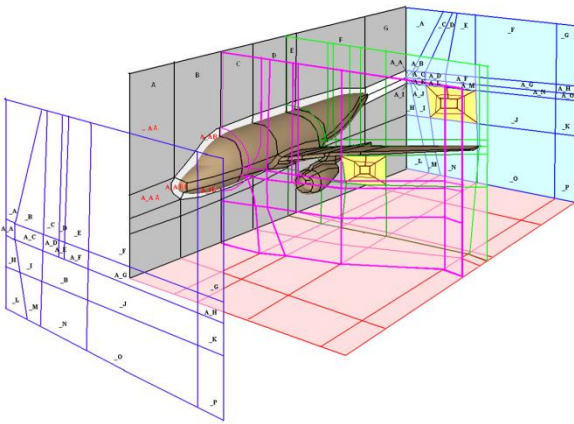


Fig. 3. Block structure near the model in the Transonic Wind Tunnel

The space around open test section of the low-speed WT T-104 is more variform. The airplane model is placed over a platform (experimental table), which, in this case, imitates a land (Fig. 4). So, the block structure is more complicated (Fig. 5).



Fig. 4. General view of the WT T-104

All dimensions used in the problem match the available drawings as closely as possible. Inside the calculation blocks, an adapted grid, which is condensed in those places, where large flow gradients are expected, is constructed - for example, at the edges of the wings.

For each cell, we determine the volume, area, coordinates of the center, normal vectors of faces, etc. The boundary conditions are set on the boundaries of the calculation region. Some of them are written in the standard way, for example, the no-slip condition at solid surfaces. The other part has a specific form, characteristic only for the given problem.

For example, the condition of the “treadmill” is formulated by analogy with the condition of the flow slipping with a given velocity. Particular attention is paid to specifying the levels and scales of turbulence at the entrance to the test section of the WT. This makes it possible to expect that in the case of the correct description of the flow gradients in the tunnel, the levels and scales of turbulence in the model installation will correspond to the reality at least in the order of magnitude. The set of special boundary conditions includes algorithms of modeling the flow near the boundaries with perforation and the so-called slotted walls. There are two sets of parameters with and without taking into account the flow in the WT plenum chamber.

3. Computational method

3.1. Explicit scheme. Global, local and fractional time stepping

Let's consider following scalar non-linear model equation of general form:

$$\frac{\partial u}{\partial t} + \frac{\partial F(u)}{\partial x} = 0. \quad (1)$$

For simplicity, let's consider a uniform grid with steps h , τ . For a start, let's consider an explicit scheme of the second order in time that is used by authors for numerical solution of Euler and Reynolds equations. In this scheme, the time step is performed using two-step procedure like "predictor-corrector". It may be considered as an explicit two-step Rounge-Kutta procedure – Euler method with central point:

$$\begin{cases} \frac{\tilde{u}_i^{n+1} - u_i^n}{\tau_n} + \frac{F_{i+1/2}(u^n) - F_{i-1/2}(u^n)}{h_i} = 0, \\ u_i^* = \frac{u_i^n + \tilde{u}_i^{n+1}}{2}, \\ \frac{u_i^{n+1} - u_i^n}{\tau_n} + \frac{F_{i+1/2}(u^*) - F_{i-1/2}(u^*)}{h_i} = 0. \end{cases} \quad (2)$$

Here, i is a number of calculation cell in space. Half-integer indices correspond to sides of calculation cell. n is time step number, h_i is grid step in space (cell size), τ_n is a time step value. The used scheme belongs to Godunov-type scheme class. Therefore, to calculate parameters on sides of cells, a Riemann problem solution about decay of an arbitrary discontinuity is used:

$$F_{i+1/2}(u) = F(U_{i+1/2}), U_{i+1/2} = \text{Decay}(u_L, u_R). \quad (3)$$

To achieve the second approximation order in space, a linear reconstruction of space distribution of parameters over cell is used:

$$u_L = u_i + \left(\frac{\partial u}{\partial x}\right)_i \frac{h_i}{2}, u_R = u_{i+1} - \left(\frac{\partial u}{\partial x}\right)_{i+1} \frac{h_{i+1}}{2}, \quad (4)$$

To calculate gradients of parameters in the cells, minimal derivative principle that guaranties

TVD-property of scheme is used. Details can be found in [9].

Such explicit scheme is stable, when time step τ satisfies to know CFL condition:

$$\text{CFL} \equiv \left| \frac{dF}{du} \right| \frac{\tau_n}{h_i} \leq 1. \quad (5)$$

Advantages of scheme (2) - (4) are clear physical sense and small errors of the method. They make this scheme optimal for high-quality description of non-stationary processes. However, attempts to use this scheme for description of flow with turbulent boundary layers show that it is ineffective because its conditional stability results in too slow motion in time.

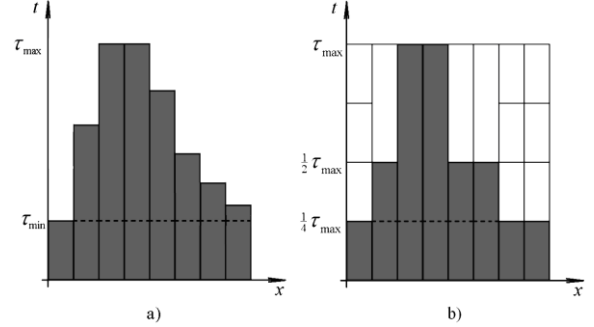


Fig. 6. To explanation of global, local and fractional time stepping

A standard approach for time stepping organization (*global time stepping*) is following. The most rigid condition for time step is chosen and time step $\tau_i = \tau_{\min}$ is performed in all the cells (Fig. 6, a). Let's $\tau_{\min} \ll \tau_{\max}$. It is typical for strongly non-uniform grids that are used for simulation of flows with boundary layers. At that time, Courant number $\text{CFL}_i \ll 1$ in most cells. Then, the information in most cells passes only small part of grid step h_i per time step. Therefore, the information propagates very slowly over the computational domain and a lot of time steps are necessary to describe the characteristic interval of global flow changing. This is the *problem of small time steps*. To the contrary, implicit scheme, *in principle*, permits to perform the calculation with arbitrarily large values of time steps and, accordingly, to achieve the result immeasurably faster. It is this factor that makes implicit schemes so popular.

But, as it is shown in [9], the payment for the velocity of result obtaining is loss of quality of non-stationary process description. There are some methods to accelerate the calculation, in the case of explicit approach to approximation of equations.

When a stationary flow is calculated using time-marching method, we aren't interested in a quality of intermediate non-stationary process description. Only its convergence to a correct stationary state is important. In this case, different methods of convergence acceleration may be used. One of them is a *method of local time stepping*. It is known approach (see, for example, [14]). In this case, the calculation in each cell is performed with time step that is defined by local restrictions in this cell (Fig.6, a). As a result, time step value changes from one cell to another. But when all the parameters u_i^{n+1} are given, they are formally prescribed to the same time layer. Later on, this procedure is repeated up to the moment, when a stationary solution is achieved. In using this procedure, convergence to stationary solution accelerates essentially, because maximal possible value of time step is taken in each cell, $CFL_i \sim 1$, and the information transfers maximal possible distance ($\sim h_i$) per time step. Thus, the flow faster adapts to the stationary boundary conditions. It is easy to understand that the number of time steps should be $O(\tau_{\max} / \tau_{\min})$ times less in comparison with global stepping.

The other widely propagated method to accelerate convergence to stationary solution is multigrid method [14]. If non-stationary flow is calculated and it is important to describe each moment of this flow development correctly, then neither local time stepping nor multigrid method are acceptable. In the current work, a *method of fractional time stepping* is assumed to be used in this case.

The idea of fractional time stepping is that the calculation in each cell is performed with the most time step (i.e. with maximal possible Courant number). But the numbers of *interim time steps* are different in different cells and they are chosen so as all the cells achieve the

same layer of physical time in some moments (Fig.6, b). When the same time layer is achieved, let's name it as a completion of *global time step*. For example, if a *interim* time step in the cell A is equal to τ_{\max} , in B - $\tau_{\max} / 2$ and in C - $\tau_{\max} / 8$, then, during one *global* time step, one should perform one *interim* time step in the cell A, two *interim* time steps in the cell B and eight *interim* time steps in the cell C. Therefore, the *global* time step in each cell is divided (*fragmented*) into smaller *interim* time steps so as the *interim* time steps satisfy to the local restriction on time step in the given cell. That's why the procedure is named as *fractional time stepping*.

It should be noted that the first description of such method that is known by authors was given in the article [15].

3.2. Implicit scheme. Dual-time stepping

Now the most propagated method to solve the problem of small time step is the use of implicit schemes. Let's take the same model equation for example and describe the implicit scheme. The scheme that satisfies following requirements has been chosen:

1. The scheme for steady calculations can be low (first) order approximation at time. That is, this scheme can have simplified implicit operator, i.e. linearized implicit operator.
2. The scheme for unsteady calculations is to be "time-accurate", i.e. it has to be of the second order approximation at least (used schemes have the second order approximation in space). In addition, these schemes haven't to simplify of implicit operator, i.e. the implicit operator isn't linearized, doesn't split into space directions or into physical processes and so on.
3. The approximation of the space operator in scheme has to be based on the same principles as the corresponding approximation in the explicit scheme.

For the model equation (1), "unsteady" implicit scheme is formulated as follows:

$$\begin{aligned} & \left(1 + \frac{\tau_n}{\tau_{n-1} + \tau_n} \right) \frac{u_i^{n+1} - u_i^n}{\tau_n} - \\ & - \frac{\tau_n}{\tau_{n-1} + \tau_n} \frac{u_i^n - u_i^{n-1}}{\tau_{n-1}} + \\ & + \frac{F_{i+1/2}(u^{n+1}) - F_{i-1/2}(u^{n+1})}{h_i} = 0 \end{aligned} \quad (6)$$

In approximating the space fluxes, the same formulas (3), (4) as in the explicit scheme are used, but parameters from the implicit (unknown) time layer ($n+1$) are substituted into these formulas. Three-layer approximation that ensures the second approximation order in time is written for time derivative. In the linear case, it can be proved that the scheme (6) is absolutely stable. Formally, the time step τ_n may be arbitrarily large ($CFL \gg 1$). It permits to essentially accelerate the calculation in near-wall zone of boundary layers in comparison with the explicit scheme. But, at that, a clear physical interpretation of the scheme losses and the values of specific errors essentially increase in comparison with the explicit scheme [9].

The main difficulty in using such implicit scheme is to solve the discrete equation (6). Because the space fluxes are approximated at the implicit time layer and they use, at that, the information from neighboring cells, then the equation for the current cell proves to be connected with the equations for neighboring cells. Hence, we obtain a system of non-linear algebraic equation (6), where the number of equations is equal to the number of the cells in “implicit” zone.

Different approaches to solution of such non-linear equation system are possible, for example, with the aid of Newton’s method. But Newton’s method, along with the most of other exact iterative methods for solution of large non-linear equation system, requires in vast resources of RAM (it is necessary to store in RAM the matrix $\frac{\partial \vec{R}}{\partial \vec{u}}$ of size $N \times N$ - the matrix with rarefied strip that has the width about $N^{2/3}$ and contains 105 non-zero diagonals in 3D case) and in vast calculation time (costs per iteration

are very large: the matrix $\frac{\partial \vec{R}}{\partial \vec{u}}$ is calculated at each iteration again, then it is inverted and multiplied by the vector \vec{R}). In addition, it can be that the iterations don’t converge.

That’s why, a **dual-time stepping method** is usually used for realization of time-accurate implicit scheme instead of traditional methods for solving large non-linear algebraic equation systems. In the case of such approach, a fictitious non-stationary term is added to the discrete equation (6):

$$\begin{aligned} & \frac{\partial u}{\partial \xi} + \left(1 + \frac{\tau_n}{\tau_{n-1} + \tau_n} \right) \frac{u - u_i^n}{\tau_n} - \\ & - \frac{\tau_n}{\tau_{n-1} + \tau_n} \frac{u_i^n - u_i^{n-1}}{\tau_{n-1}} + \\ & + \frac{F_{i+1/2}(u) - F_{i-1/2}(u)}{h_i} = 0 \end{aligned} \quad (7)$$

Here, ξ is pseudo-time. The idea is following. The stationary solution of the problem (7), when it is single, coincides with the solution of the discrete equation (6): in the stationary limit $u = u^{n+1}$. It permits to solve the equation (6) by method of marching along pseudo-time. The solution of the equation (6) can be achieved as a limit of developing the pseudo-non-stationary process that is described by the equation (7).

Because it is time-marching method and we are interested in a stationary solution only, then different methods of convergence acceleration may be used to obtain this solution.

One of the first realizations of dual-time stepping method, which was proposed by E.Jameson [14], used the explicit method of marching along pseudo-time. To accelerate the convergence to the stationary solution (i.e. to solution at the implicit physical time layer $n+1$ – see (6)), a local time stepping method is used. Thus, some thousands of pseudo-time steps are to be performed for one step of physical time. Instead, an implicit scheme with global pseudo-time stepping is used for description of pseudo-time stabilization process. Because we are interested in stationary solutions of the equation (7) only, one may use high-efficient implicit

schemes with strongly simplified implicit operator that are widely used now for solution of stationary problems. Here, a possible example of such hyper-fast scheme is presented:

$$\left\{ \begin{array}{l} u_i^{(0)} = u_i^n, \\ \frac{u_i^{(k+1)} - u_i^{(k)}}{\Delta \xi} + \frac{3}{2} \frac{u_i^{(k+1)} - u_i^n}{\tau} - \frac{1}{2} \frac{u_i^n - u_i^{n-1}}{\tau} + \\ + \frac{A_{i+1/2} \cdot [\tilde{U}_{i+1/2}^{(k+1)} - \tilde{U}_{i+1/2}^{(k)}] - A_{i-1/2} \cdot [\tilde{U}_{i-1/2}^{(k+1)} - \tilde{U}_{i-1/2}^{(k)}]}{h} + \\ + \frac{F_{i+1/2}(u^{(k)}) - F_{i-1/2}(u^{(k)})}{h} = 0, \quad k = 1, \dots, M, \\ u_i^{n+1} = u_i^{(M)}. \end{array} \right. \quad (9)$$

Such scheme has only the first order in pseudo-time that results both in calculation acceleration and in improvement of its stability. The implicit part of space operator in the equation (9) has been obtained using linearization of space operator in the equation (7) and it has only the first approximation order as pseudo-time derivative approximation. Jacobians $A_{i+1/2} = A(u_i^n, u_{i+1}^n)$ are calculated only once during the stabilization time. Let's draw attention that the non-linear approximation of the second order is used as before for the explicit part of the space operator.

The formula (9) results in a system of linear algebraic equations for all the cells of computational domain. This system has banded matrix (its non-zero elements are aggregated near the main diagonal of the matrix). But, in the case of 3D problems, this band of non-zero elements is a quite wide, in spite of its essential rarefaction (it contains 9 non-zero diagonals only and there are wide zero bands between the diagonals). The elements of non-zero diagonals are fully filled blocks of size 7x7 (it corresponds to 7 equations of conservation of mass, impulse, energy and turbulence parameters that are written for each cell). In spite of the wide non-zero band of this banded matrix, this implicit scheme doesn't require essential costs of RAM, because modified Gauss-Seidel method for block-diagonal matrices [16] is used to solve this system. Instead of exact solution of linear equation system (9), only 6 iterations of Gauss-

Seidel method are performed. It is acceptable because the exact solution isn't necessary at each pseudo-time step; it is necessary only to the moment, when the stationary solution is achieved. In approaching to the stationary solution, the parameters become pseudo-time-independent and 6 iterations of Gauss-Seidel method becomes sufficient to obtain an exact solution of the system (9).

3.3. Boundary conditions

Let's consider some special boundary conditions.

Connect is the boundary condition describing common boundary neighboring blocks of the computational domain on which the continuity of grid lines is violated. In this case the parameters at the outer side of the boundary are found by interpolation of the parameters from the near-boundary cells of the neighboring block.

Tunnel In-Out is the boundary condition required to obtain the correct values of the Mach number in the control point of a wind tunnel. The peculiarity of the problem is that the input parameters are set inflexibly because they are introduced from the virtual control panel of the computational WT. Usually these parameters are the Mach number M_{entr} , full pressure of the fore-chamber full temperature of gas of the fore-chamber and the area of the entry section S_{entr} .

Darcy is the boundary condition that allows simulation of WT with perforated walls. It is known that in the case of small pressure differences across the porous surface the Darcy law holds [17], which postulates that on the control surface the gas velocity normal to the perforated wall (the effective velocity of the flow through the perforation holes) is directly proportional to the difference of the static pressure across the wall. In the case of small perturbations, it is possible to use a simplified system of the Euler equations in the linear form and the problem of the decay of an arbitrary discontinuity can be solved in the acoustic approximation. It is assumed that the perforated wall separates the basic flow from the WT

plenum chamber in which gas is practically motionless.

4. EWT as a part of experimental cycle

4.1. European Transonic Wind Tunnel

In this section an example of the construction of a rather complicated mathematical model WT, having slotted boundaries, which separate the test section from the plenum chamber, is considered. The overall view of such a WT (European Transonic Wind Tunnel (ETW)) is given in the photograph, see Fig. 7 (back view).

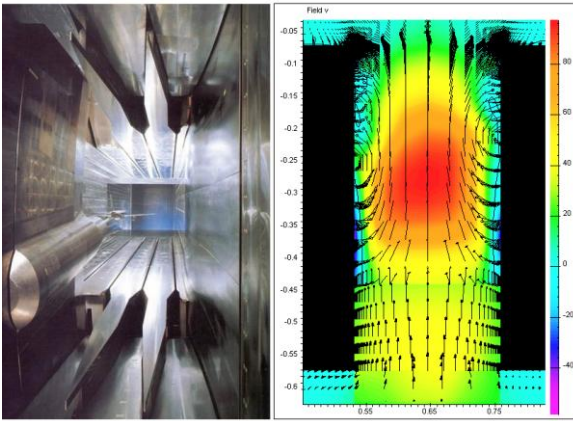


Fig. 7. Photograph of ETW and flowfield in slot

The lower wall with slots, shaped side wall, movable leaf in the WT mixing area (teeth at the center of the photo), and support with the model are seen. This WT operates in different modes. As a rule, tests are carried out in the nitrogen medium at a temperature of 100 K. It is possible to carry out studies with the use of air at a usual temperature of about 280 K. These modes are of the greatest interest for this work. Another photo showing the location of the airplane model on the support is given in Fig.2. The photo clearly shows the longitudinal slots in the walls, the fin sting with the crescent of the alpha mechanism, and the blade for turn of the flow at the end of the channel. The WT test section is surrounded by the plenum chamber, which has a large diameter (6 m) and serves to equalize the main flow. A feature of this mathematical model is that the slots in the WT walls have an extremely small width and, despite this, have

the utmost influence on the stream in the flow core. From this viewpoint, the considered problem has a substantially different linear scale, which makes its solution more difficult. The starting data necessary for the work have been presented by J. Quest (ETW) as text files. The files had coordinates of flat projections and cross sections of the basic elements of the WT's test section, as well as formulas describing the characteristic features of the fragments of particular details. Attention should be paid to the relationship of the slot width and width of WT walls. The width of one slot is $l = 25$ mm and WT width is $L = 2400$ mm. In addition, the slots have a complicated form and are cut in the metallic plate of $d = 450$ mm in thickness. In the plenum chamber, they have a width of $lp = 90$ mm and contact with a nonmobile flow. In the construction of the mathematical model, part of the information is left out, for example, the curving of slot fringes is not taken into account. The cross section of the test section entrance is a rectangle 2000 mm high and 2400 mm wide. The lower panel is inclined downwards at an angle of $\delta = -0.55^\circ$ relative to the axis passing through the given point. A significant role in the tests is played by the α -mechanism of the crescent, which exerts a strong influence on the results. The crescent is designed so that during a change in the angle of attack, the turning point of the model remains stationary. The fore edge of the crescent is rounded and the rear is elliptical and is defined by the formula $y^2 = b^2(a^2 - x^2)/a^2$, where a and b are ellipse's semiaxes. The ellipse is interfaced with the contour of the central body on a tangent. The geometry of the central body is simplified without accounting for the rounding of the edges. A separate element of the design is the rotary valve located in the area of the WT's reentry. It is clearly seen in Fig. 7 as an element which cuts into the teeth. The rotary valve has the ability to rotate. The front part of the valve is bent down. It creates a smooth junction of channels formed by slots with the mixing zone in ETW.

To carry out the calculation, a multiblock grid is constructed. In the simplest case, it has (for a quarter) 27 blocks. One block is in the plenum chamber; three blocks are in the area of

the plenum chamber docking with slots, with one block in each slot; one block is in the part of the reentry; and one block is in the area of the pier and support of the model. Before the entrance into the test section of the WT and in the exit from it, additional blocks are placed to state the boundary conditions. The computational grid condenses in the designated areas to improve the approximation of the solution. Along the slot length, 110 cells are placed, and 50 cells are placed across it. Between the slots, 40 cells are placed. Even in the case of the totally closing of the slots, the plenum chamber is not overlapped completely. It allows one to model the flow near reentry. The mathematical model of ETW is necessary in order to understand the physical features of the flow in the test section and to fill in the missing experimental data, for example, to consider the scale effect of the model or to subtract the effect of the WT (WT walls, etc.) from the results of the experiment. The calculation shows that despite the considerable size of the WT (in this case, the test section blockage was estimated at 3%), turbulence from the model reach all walls and penetrate inside the plenum chamber. We consider the cross section of the central slot on the low wall near the reentry (see Fig. 7). The flow is highly turbulent and is characterized by the presence of several vortices. It is seen that the turbulence propagate not only upward (test section) but also downward (pressure chamber). The calculations show that a weak flow is formed in the plenum chamber directed opposite to the basic flow in the test section. This flow is expelled into the test section at the origin of the slot, which leads to the test section formation of low-frequency pulsations. Thus, the mathematical WT model becomes an obligatory part of the technology of the physical experiment in the wind tunnel.

4.2. TsAGI T-128

For example, the method described here is used to determine the effect of the perforated boundaries of the flow in the TsAGI WT T-128. The photograph of T-128 test section is shown in Fig. 8.



Fig. 8. Photograph of T-128 test section

Figure 9 compares the calculation and experimental results on the upper wall of the WT test section.

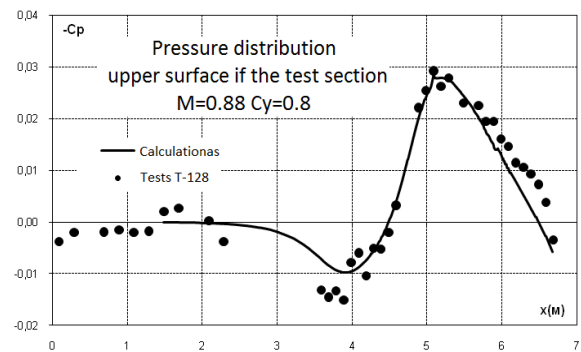


Fig. 9. Comparison of the pressure coefficient distribution on the test section upper surface

Good convergence of the pressure coefficient, which is observed in the figure, is a necessary condition for the accuracy of the results of the numerical calculation. The available methods to take into account the influence of the flow boundaries in T-128 permit us to determine the corrections to the parameters of the incoming flow (to the attack angle, Mach number and velocity pressure) by the results of the numerical studies, as well as to determine the results of the measurement by a strain-gauge balance of the loads acting on the model (drag, lift and pitching moment coefficients). An important field for the application of the described approach in the procedure of aerodynamic tests is the determination of the influence of supporting devices. In the experimental method of doubling the suspenders, it is very difficult to exclude the

interference of the basic supporting device and the imitator of the other device. In the application of the calculation methods, this problem is absent. The numerical methods are very important in designing the aerodynamic contours of the supporting devices having the minimal influence on the characteristics of the models under investigation. Thus, for example, Figure 10 shows the distribution of longitudinal component of the velocity fluctuations (Mach number) about the surface of the wing caused by the effect of three configurations of the fin sting shown in Fig. 11.

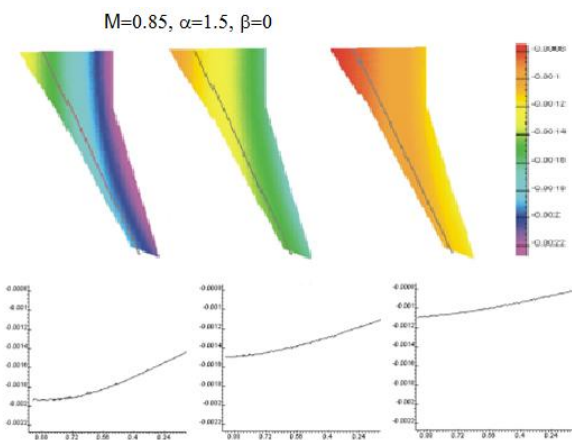


Fig. 10. Distribution of the longitudinal velocity fluctuations for different sting positions in T-128

Minimization of the turbulent components of velocity and their gradients on the model surface makes it possible to design an optimal supporting device.

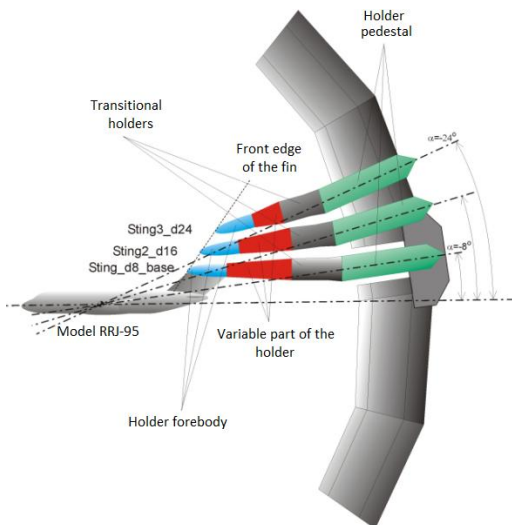


Fig. 11. Three positions of the sting in T-128

4.3. TsAGI T-104

Let's describe a procedure of engine model testing in T-104 Wind Tunnel. To supply to the engine a special pylon is used that is installed under the engine model (Fig. 12).

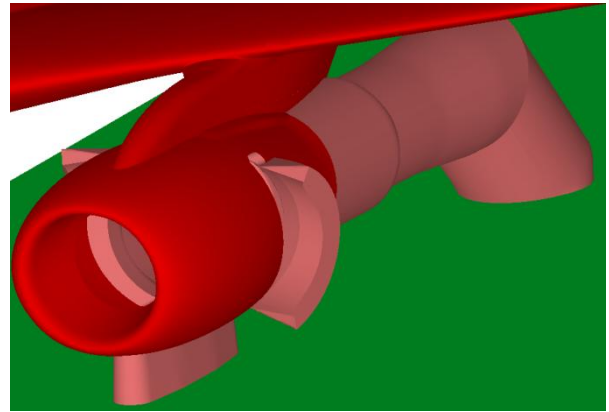


Fig. 12. Model of the engine with pylon and ejector

The engine mode is regulated by the ejector (a tube at the nozzle exit). These elements are sufficiently large and can influence the experimental results. To estimate this influence, we carry out the calculation in two configurations: a) with pylon and ejector, b) without them. We assume that the "reverse thrust" device works. The jet is visualized by measuring the temperature fields. Let's consider the "velocity cutoff" mode of reinjection jets. It is determined by the free stream Mach number at which reversed flow sucked into the engine inlet. In the tests, this mode is determined by the temperature sensors, in the calculation – by streamlines and temperature fields (jet is warmed up), as shown in Fig. 13.

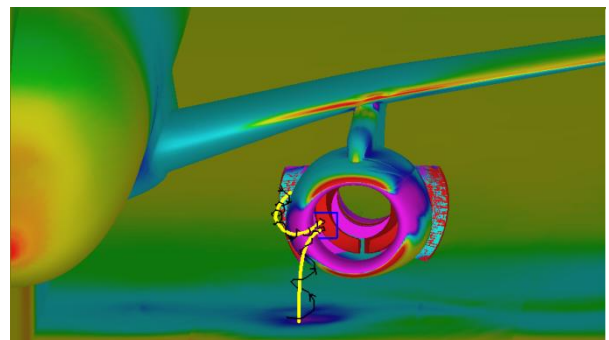


Fig. 13. Flow in the case of reinjection

The calculated data show that the pylon due to excessive back pressure "pushes" the stream from the entrance to the engine and reinjection occurs at higher Mach numbers than without pylon. This means that the experimental data may contain errors in the determination of the "velocity cutoff" mode of flow with the thrust reversers, as the pylon is an integral part of the experimental setup. But in this experiment, there is another important factor, which is also impossible to simulate in T-104 WT – the presence of running land. This part of the experiment can be fulfilled by the calculation with a special boundary condition. The results of such calculations with boundary condition "treadmill" one can see in Fig. 14.

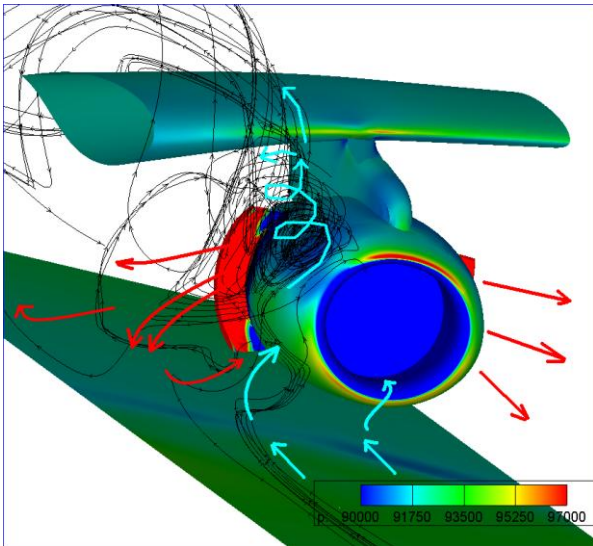


Fig. 14. Influence of the treadmill to reinjection

The analysis shows that in the case of a fixed screen, reinjection begins earlier. Thus, we obtained an interesting result. Two effects (the influence of the pylon and the treadmill), which cannot be simulated in this experiment, give an opposite contribution to the outcome of the experiment and almost cancel each other out.

Thus, the mathematical model of the WT is an integral part of the methodology of experimental research in wind tunnels.

References

[1] Vaganov A.V., Glazkov S.A., Neyland V.M., Semenov A.V. Some Features of the Method of

Testing in a Wind Tunnel with Sectional-Controlled Adaptive Perforation of the Test Section of Walls. *Soviet-French Subgroup on Aerodynamics, Aviation Acoustics and Elasticity, Paris, 1990.*

[2] Velichko Yu.D., Lifshiyz S.A. AIRFOIL. A Computer Codes Library for Numerical Analysis of Viscous Transonic Flow around a Wing Section. *La Recherche Aerospaciale. 1994.*

[3] Neyland V.M., Ivanov A.I., Semenov A.V., Semenova O.K., Amirjanz G.A. *AGARD-CP-585. October 1996.*

[4] Gorbushin A.R., Ivanov A.I., Khozyaenko N.N. Two Methods for Study of Boundary Conditions on Permeable Walls of Transonic Wind Tunnels. *4th All-Union School in Methods for Aerophysical Studies [in Russian]. 1986.*

[5] Glazkov S.A., Gorbushin A.R., Khozyaenko N.N. Determination of Flow Characteristics of Perforated Panels. *Uch. Zap. TsAGI. 1982, Vol. XIII, 4.*

[6] Semenov A.V., Semenova O.K. The Influence of the Boundaries of the Work Part of a Wind Tunnel with Rigid Side and Perforated Horizontal Walls. *Uch. Zap. TsAGI. 1986, Vol. XVII, 3.*

[7] Glazkov S.A., Ivanova V.M. A Study of the Induction of Permeable Walls of a Wind Tunnel by Known Parameters of the Near Flow. *Uch. Zap. TsAGI. 1982, Vol. XIII, 4.*

[8] Bosnyakov S.M., Akinfiyev V.O., Vlasenko V.V., Glazkov S.A., Lysenkov A.V., Matyash S.V., Mikhailov S.V. Methods of Numerical Simulation of Flows Past Models in Wind Tunnels and an Attempt at Its Practical Application. Parts 1 and 2. *Tekhn. Vozd. Flot. 2006, Vol. 80, 5, 6.*

[9] Bosnyakov S., Kursakov I., Lysenkov A., Matyash S., Mikhailov S., Vlasenko V., Quest J. Computational Tools for Supporting the Testing of Civil Aircraft Configurations in Wind Tunnels. *Progr. Aerospace Sci. 2008, Vol. 44, 2, pp. 67-120.*

[10] Glazkov S.A., Gorbushin A.R., Ivanov A.I., Semenov A.V. Recent Experience in Improving the Accuracy of Wall Interference Corrections in TsAGI T-28 Wind Tunnel. *Progr. Aerospace Sci. 2001, Vol. 37, 3.*

[11] Melber-Wilkending S., Heidebrecht A., Wichmann G. A New Approach in CFD Supported Wind Tunnel Testing. *25th Int. Congr. of the Aeronautical Sciences, ICAS. 2006.*

[12] Collercandy R., Marques B., Lory J., Dbjay S., Espiau L. Application of CFD for Wall and String Effects. *HiReTT Report HIRETTT NAFRCo WP 2.2311002003. October 2003.*

[13] Coons, S. Surfaces for Computer Aided Design of Space Forms. *Report MAC TR 41, Project MAC, M.I.T. 1967.*

- [14] Jameson, A. A perspective on computational algorithms for aerodynamic analysis and design. *Progress in Aerospace Sciences*. 2001, Vol. 37, 2.
- [15] Pervaiz M.M., Baron J.R. Spatiotemporal adaptation algorithm for two-dimensional reacting flows. *AIAA Journal*. 1989, Vol. 27, 10.

Copyright Statement

The authors confirm that they, and/or their company or organization, hold copyright on all of the original material included in this paper. The authors also confirm that they have obtained permission, from the copyright holder of any third party material included in this paper, to publish it as part of their paper. The authors confirm that they give permission, or have obtained permission from the copyright holder of this paper, for the publication and distribution of this paper as part of the ICAS2012 proceedings or as individual off-prints from the proceedings.